

The Hexaazidosilicate(IV) Ion: Synthesis, Properties, and Molecular Structure

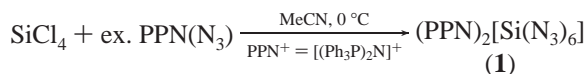
Alexander C. Filippou,* Peter Portius, and Gregor Schnakenburg

Humboldt-Universität zu Berlin, Institut für Chemie, Brook-Taylor-Strasse 2, 12489 Berlin, Germany

Received June 17, 2002

Binary azides of group 14 elements form a class of rare highly endothermic compounds.¹ Synthesis and handling of these compounds afford proper experimental care to minimize unpredictable, explosive hazards resulting from exothermic decomposition by elimination of dinitrogen.² Therefore, it is not surprising that to date only the ions $[\text{C}(\text{N}_3)_3]^+$ ³ and $[\text{E}(\text{N}_3)_6]^{2-}$ ($\text{E} = \text{Ge-Pb}$)^{1,4} and the primary explosive $\alpha\text{-Pb}(\text{N}_3)_2$ ⁵ have been isolated and structurally characterized. In comparison, structural information for analogous silicon compounds is lacking. Thus far, only $\text{Si}(\text{N}_3)_4$ has been reported to be a violently explosive substance,⁶ which was prepared in situ and characterized by ²⁹Si NMR or IR spectroscopy.⁷ Following our interest in main-group element azides with a high nitrogen content,⁸ we describe here the synthesis and full characterization of the $[\text{Si}(\text{N}_3)_6]^{2-}$ ion.

Treatment of a solution of SiCl_4 in CH_3CN with an excess of $(\text{PPN})\text{N}_3$ at 0 °C leads selectively to $(\text{PPN})_2[\text{Si}(\text{N}_3)_6]$ (**1**) as evidenced by IR monitoring of the reaction (equation).



The hexaazidosilicate salt **1** was separated from $(\text{PPN})\text{X}$ ($\text{X} = \text{Cl}, \text{N}_3$) after repeated recrystallization from CH_3CN and isolated as a colorless, moisture-sensitive, crystalline solid in 37–62% yields. It was characterized by elemental analysis, thermal analysis and IR, Raman, ²⁹Si, and ¹⁴N NMR spectroscopies and single-crystal X-ray crystallography.⁹ Compound **1** is insoluble in THF and very soluble in CH_2Cl_2 and CH_3CN to give colorless solutions, which turn immediately cloudy due to hydrolysis, when exposed to air. Hydrolysis of **1** liberates HN_3 and $(\text{PPN})\text{N}_3$.¹⁰ The hexaazidosilicate salt **1** exhibits remarkable thermal stability, melting in vacuo without decomposition at 225 °C. Its melting point is even higher than that of the germanium analogue $(\text{PPN})_2[\text{Ge}(\text{N}_3)_6]$ (**2**) (mp = 211 °C).¹ Simultaneous thermal analysis (TG-DTA) of **1** coupled with mass spectrometric detection of the evolved gases revealed that two distinct exothermic decomposition processes follow the endothermic melting of **1** at the extrapolated onset temperature $T_{\text{on}}^{\text{ex}} = 214$ °C (peak temperature $T_p = 220$ °C). The first process started at $T_{\text{on}} = 256$ °C ($T_p = 296$ °C) and was associated with a mass loss of 6.1%, which is mainly ascribed to elimination of N_2 .¹¹ The second process was observed at $T_{\text{on}} = 321$ °C, and was accompanied by a fast mass loss and liberation of energy ($T_p = 333$ °C) leading to a pressure surge on the balance. This process involves degradation of the PPN cations and evolution of $\text{Si}(\text{N}_3)_4$, N_2 , and some HN_3 .¹¹ The solid-state structure of **1** was determined by single-crystal X-ray diffraction. **1** crystallizes in the space group $P\bar{1}$ and is isostructural with the hexaazidogermanate salt **2**.¹ The crystal structure of **1** consists of discrete PPN^+ cations and S_2 symmetric $[\text{Si}(\text{N}_3)_6]^{2-}$ anions (Figure 1). The mean $\text{Si-N}_{\text{azide}}$ bond length of **1** (1.871 Å,

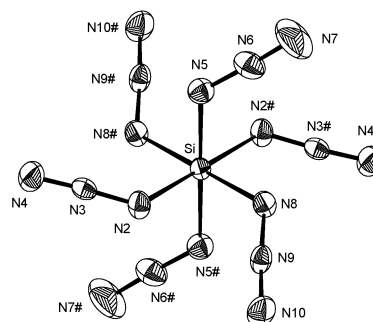


Figure 1. DIAMOND plot of the anion $[\text{Si}(\text{N}_3)_6]^{2-}$ in **1** (view down the pseudo- S_6 axis). Thermal ellipsoids are set at the 50% probability level. Selected bond lengths (Å) and angles (deg): Si–N2 1.866(1), Si–N5 1.881(1), Si–N8 1.867(1), N2–N3 1.198(2), N3–N4 1.144(2), N5–N6 1.201(2), N6–N7 1.144(2), N8–N9 1.207(2), N9–N10 1.146(2), Si–N2–N3 126.5(1), Si–N5–N6 122.6(1), Si–N8–N9 121.9(1), N2–Si–N5 90.16(6), N2–Si–N8 89.32(6), N5–Si–N8 90.30(6), N2–N3–N4 175.3(2), N5–N6–N7 176.4(2), N8–N9–N10 176.1(2).

Table 1) is 6–11 pm longer than those reported for tetrahedral azidosilanes ($\text{Si-N} = 1.760(3)\text{--}1.814(2)$ Å).¹² The mean $\text{N}_\alpha\text{--N}_\beta$ and $\text{N}_\beta\text{--N}_\gamma$ bond lengths in **1** (1.202 and 1.145 Å, Table 1) agree well with those in $(\text{PPN})_2[\text{Ge}(\text{N}_3)_6]$ ($(\text{N}_\alpha\text{--N}_\beta)_{\text{av}} = 1.212$ Å, $(\text{N}_\beta\text{--N}_\gamma)_{\text{av}} = 1.147$ Å)¹ and the difference $\Delta(\text{NN})$ between the N–N bond lengths of 5.7 pm is smaller than that found in other covalent azides.⁸ All of these structural parameters suggest in agreement with the IR data and the results of the theoretical calculations the presence of polar Si–N bonds in **1**. The IR spectra of **1** in CH_3CN display at different concentrations only one very strong absorption band for the $\nu_{\text{as}}(\text{N}_3)$ vibration at 2109 cm^{-1} .^{13,14} and give no evidence for a dissociation of **1** to $(\text{PPN})\text{N}_3$ and $\text{Si}(\text{N}_3)_4$.^{10,15} The Raman and IR spectra of **1** are consistent with the presence of S_6 symmetric $[\text{Si}(\text{N}_3)_6]^{2-}$ ions in solution and allow in combination with the calculated vibrational spectra (Supporting Information) an assignment of most observed bands to fundamental modes of the $[\text{Si}(\text{N}_3)_6]^{2-}$ ion.⁹ The ²⁹Si NMR spectrum of **1** in CH_3CN displays one sharp signal at $\delta = -188.7$ ppm,¹⁶ which is considerably upfield-shifted relative to that of $\text{Si}(\text{N}_3)_4$ (-75.1 ppm).^{7a} The ²⁹Si chemical shift of **1** agrees well with that calculated for the $[\text{Si}(\text{N}_3)_6]^{2-}$ ion (-198.2 ppm)¹⁶ using the GIAO-MBPT(2) method,¹⁷ and is similar to that reported for other hexa-coordinate silicon compounds, such as ZnSiF_6 ($\delta = -185.3$ ppm).¹⁸ All these facts provide additional evidence for the presence of intact $[\text{Si}(\text{N}_3)_6]^{2-}$ ions in solution. The ¹⁴N NMR spectrum of **1** in CH_3CN shows two singlet resonances at $\delta = -214.7$ (N_γ) and -297 ppm (N_α) for the $[\text{Si}(\text{N}_3)_6]^{2-}$ ion, which agree well with the calculated values ($\delta(\text{N}_\gamma/\text{N}_\alpha) = -217/285$ ppm).^{16,19}

The electronic structure of the $[\text{Si}(\text{N}_3)_6]^{2-}$ ion was calculated using different methods and basis sets (Table 1, Supporting Information).^{20,21} All geometry optimizations led to a S_6 symmetric minimum structure as the most stable $[\text{Si}(\text{N}_3)_6]^{2-}$ isomer. Moreover, a good to excellent agreement was found between the calculated and experimental bond lengths and angles.

* To whom correspondence should be addressed. E-mail: filippou@chemie.hu-berlin.de.

Table 1. Experimental and Calculated Parameters of $[\text{Si}(\text{N}_3)_6]^{2-}$ ^a

	bond lengths D [Å]			angles [°]
	Si–N _α	N _α –N _β	N _β –N _γ	Si–N _α –N _β
X-ray ^b	1.871(5)	1.202(3)	1.145(1)	124(1)
RI-MP2/TZVP	1.876	1.206	1.174	126.1
RI–BP86/TZVPP ^c	1.902	1.205	1.161	127.2
B3LYP/TZVPP ^c	1.896	1.195	1.146	127.1
HF/TZVPP ^c	1.889	1.179	1.108	124.4
	partial charges q [e]			
BP86/TZVPP	Si: +1.86	N _α : –0.58	N _β : +0.22	N _γ : –0.28

^a Details of all theoretical calculations are found in the Supporting Information. ^b The unweighted mean x_u of the three crystallographically independent bond lengths and angles of **1** is listed. The standard deviation σ of x_u is given in parentheses and was calculated by $\sigma^2 = \sum(x_i - x_u)^2/(n^2 - n)$, x_i = individual value, $n = 3$. ^c Restrained geometry (S_6).

The best results were obtained at the RI-MP2/TZVP level (Table 1). The small difference between the calculated and experimental N_{β} – N_{γ} length ($D_c = 1.174$, $D_o = 1.145(1)$ Å) can be traced back to thermal motion in the crystal.²² Thus, a correction of D_o with the riding model²² led to a significant elongation of the N_{β} – N_{γ} distances ($D_i(\text{av}) = 1.166(5)$ Å),²³ which agrees very well with the calculated length, whereas the Hirshfeld test for rigid body vibrations²⁴ failed with the X-ray data of **1**.²⁵ An NBO analysis of $[\text{Si}(\text{N}_3)_6]^{2-}$ reveals the presence of polar Si–N bonds (Table 1).²⁶ A second isomer of $[\text{Si}(\text{N}_3)_6]^{2-}$ with D_{3d} symmetry was also found to be a local minimum on the potential energy surface. However, this isomer is less stable than the S_6 symmetric isomer (100.3 kJ mol^{–1} at the HF/SVP level and 54.4 kJ mol^{–1} at the BP86/SVP level (zero-point vibrational energy corrected). A look at the electron density distribution suggests that an optimal orientation of the azido groups is achieved in the S_6 symmetric minimum structure to minimize the Coulombic repulsion between the lone pairs of the N_α atoms and to maximize the Coulombic attraction between the opposite charged N_α and N_β atoms in adjacent azido groups.

The anion $[\text{Si}(\text{N}_3)_6]^{2-}$ belongs to a class of very rare hypercoordinate silicon complexes with a SiN₆ coordination polyhedron,^{18,27} and has the highest nitrogen content (89.98%) among the homoleptic hexaazidometalates reported thus far.²⁸ Further studies in this direction show that stable neutral Lewis-base adducts of $\text{Si}(\text{N}_3)_4$ are also accessible following a similar approach.

Supporting Information Available: CCDC 192397 contains the supplementary crystallographic data for this paper. These data can be obtained free of charge via <http://www.ccdc.cam.ac.uk/conts/retrieving.html> (or from the CCDC, 12 Union Road, Cambridge CB2 1EZ, UK; fax: +44 1223 336033; e-mail: deposit@ccdc.cam.ac.uk). Experimental Section, X-ray crystallography of **1** (CIF), thermal analysis of **1**, electronic structure calculations, calculations of NMR chemical shifts and vibrational spectra of $[\text{Si}(\text{N}_3)_6]^{2-}$, isocharge plot of calculated and experimental electron density (PDF), and Acknowledgment. This material is available free of charge via the Internet at <http://pubs.acs.org>

References

- Filippou, A. C.; Portius, P.; Neumann, D. U.; Wehrstedt, K.-D. *Angew. Chem., Int. Ed.* **2000**, *39*, 4333 and references therein.
- Brethrick's Handbook of Reactive Chemical Hazards*, 6th ed.; Urben, P. G., Ed.; Butterworth-Heinemann: Oxford, UK, 1999.
- (a) Müller, U.; Bärmighausen, H. *Acta Crystallogr.* **1970**, *B26*, 1671. (b) Petrie, M. A.; Sheehy, J. A.; Boatz, J. A.; Rasul, G.; Prakas, G. K. S.; Olah, G. A.; Christie, K. O. *J. Am. Chem. Soc.* **1997**, *119*, 8802.
- (a) Fenske, D.; Dörner, H.-D.; Dehnicke, K. Z. *Naturforsch.* **1983**, *B38*, 1301. (b) Polborn, K.; Leidl, E.; Beck, W. Z. *Naturforsch.* **1988**, *B43*, 1206.
- Choi, C. S.; Prince, E.; Garrett, W. L. *Acta Crystallogr.* **1977**, *B33*, 3536.
- Wiberg, E.; Michaud, H. Z. *Naturforsch.* **1954**, *B9*, 500.
- (a) Herges, R.; Starck, F. J. *Am. Chem. Soc.* **1996**, *118*, 12752. (b) Maier, G.; Reisenauer, H. P.; Glatthaar, J. *Organometallics* **2000**, *19*, 4775.
- (a) Filippou, A. C.; Portius, P.; Kociok-Köhn, G.; Albrecht, V. *J. Chem. Soc., Dalton Trans.* **2000**, 1759 and references therein.
- Synthesis and spectroscopic data of **1**: A solution of SiCl_4 (0.1 mL, 0.8 mmol) in 15 mL of CH_3CN was treated at 0 °C with a solution of (PPN)- N_3 (3.47 g, 6 mmol) in 10 mL of CH_3CN . The cooling was removed and slow stirring was continued for 4 h at ambient temperature. The slightly cloudy solution was filtered at 0 °C using a stainless steel cannula fitted with a fiberglass filter (Whatman®). The clear, colorless filtrate was concentrated in vacuo below 0 °C until crystallization started, and the resulting suspension was stored for 12 h at –28 °C. The supernatant solution was decanted off and the crystalline precipitate washed with cold CH_3CN and dried for 30 min in vacuo. The recrystallization was repeated three times to afford air-sensitive, colorless crystals of **1** in 37–62% yield from SiCl_4 . Anal. Calcd for $\text{C}_7\text{H}_{60}\text{N}_{30}\text{P}_4\text{Si}$ (1357.38): C, 63.71; H, 4.45; N, 20.64. Found: C, 63.66; H, 4.37; N, 20.26%; the substance did not contain chlorine. IR (CH_3CN , cm^{-1}) $\nu = 2109$ vs ($\nu_{\text{as}}(\text{N}_3)$, E_u and A_g), 1590 vw ($\nu(\text{ar})$). IR (CH_2Cl_2 , cm^{-1}) 2108 vs ($\nu_{\text{as}}(\text{N}_3)$, E_u and A_g), 1590 vw ($\nu(\text{ar})$). IR (Nujol, cm^{-1}) 3390 vw, 3354 vw, 3055 vw, 2104 vs, 1587 vw, 1482 w, 1438 s, 1320 s, 1315 m, 1302 m(sh), 1272 m, 1184 vw, 1161 vw, 1115 s, 1026 w, 997 w, 796 w, 765 vw(sh), 750 w, 724 m, 692 s. Raman (CH_3CN , rt, cm^{-1} ; p = polarized, dp = depolarized): $\nu([\text{Si}(\text{N}_3)_6]^{2-}) = 2142$ m (p, $\nu_{\text{as}}(\text{N}_3)$, A_g), 2104 w, br (dp, $\nu_{\text{as}}(\text{N}_3)$, E_g), 2079 w, br, 1329 m (p, $\nu_{\text{sym}}(\text{N}_3)$, A_g), 1316 w (dp, $\nu_{\text{sym}}(\text{N}_3)$, E_g), 702 s (p), 440 vs (p, $\nu(\text{Si}–\text{N})$, A_g). ¹⁴N NMR (21.7 MHz, CH_3CN , rt, ppm): $\delta = -214.7$ (s, $\Delta\nu_{1/2} \approx 36$ Hz, N_{γ}), –297 (s, $\Delta\nu_{1/2} \approx 391$ Hz, N_{α}). ²⁹Si NMR (49.7 MHz, CH_3CN , rt, ppm) $\delta = -188.7$ (s, $\Delta\nu_{1/2} \approx 1$ Hz). ¹⁴N NMR of (PPN) N_3 (21.7 MHz, CH_3CN , rt, ppm) $\delta = -130.0$ (s, $\Delta\nu_{1/2} \approx 11$ Hz, N_{β}), –276.9 (s, $\Delta\nu_{1/2} \approx 28$ Hz, $2 \times N_{\alpha}$). No ¹⁴N NMR signal could be detected for the PPN cation in **1** and (PPN)X (X = Cl, N₃, solvent: CH_3CN).
- Despite all attempts for vigorous air-exclusion the IR spectra of **1** in MeCN showed always two $\nu_{\text{as}}(\text{N}_3)$ bands of varying weak intensity of the hydrolysis products HN_3 (2139 cm^{-1}) and (PPN) N_3 (2005 cm^{-1}) in addition to the strong $\nu_{\text{as}}(\text{N}_3)$ absorption band of **1** at 2109 cm^{-1} .
- At the start of the first exothermic step only the ion $[\text{N}_2]^+$ ($m/z = 28$) and to less extent the ions $[\text{N}]^+$ (14) and $[\text{HN}_3]^+$ (43) appeared in the EI mass spectra of the evolved gases. The intensity of these signals followed the progress of the DTA curve from $T_{\text{on}} = 256$ °C. The ions $[\text{Ph}]^+$ ($m/z = 77$), $[\text{Ph} - \text{C}_2\text{H}_2]^+$ (51) and $[\text{Si}(\text{N}_3)_3]^+$ (154) appeared in the mass spectra at the start of the second exothermic effect. The intensity of these signals developed as the DTA curve and increased from $T_{\text{on}} = 321$ °C to $T_p = 333$ °C. Evolution of $\text{Si}(\text{N}_3)_4$ during the second exothermic process was confirmed by an independent experiment, in which a sample of **1** was heated with a rate of 30 K min^{–1} in high vacuo and the gases analyzed with a Hewlett-Packard 5995A mass spectrometer using the EI method (70 eV, positive ions). Above 318 °C the mass spectra showed signals at $m/z = 70.1$, 154.0, and 196.1 (based on the ¹⁴N and ²⁸Si isotopes). The isotope patterns of these signals matched perfectly to those calculated for the ions $[\text{Si}(\text{N}_3)_n]^+$ ($n = 1, 3, 4$).
- (a) Zigler, S. S.; Haller, K. J.; West, R.; Gordon, M. S. *Organometallics* **1989**, *8*, 1656. (b) Denk, M.; Hayashi, R. K.; West, R. *J. Am. Chem. Soc.* **1994**, *116*, 10813.
- Two infrared active $\nu_{\text{as}}(\text{N}_3)$ modes (E_g and A_g symmetry) are expected for a S_6 symmetric $[\text{Si}(\text{N}_3)_6]^{2-}$ ion. The difference between their frequencies was calculated to be 4 cm^{-1} (BP86/DZP, effective core potential of Si; Stuttgart RLC ECP, ref 14). This suggests that the corresponding absorption bands are not resolved in the IR spectra of **1**.
- Bergner, A.; Dolg, M.; Kuechle, W.; Stoll, H.; Preuss, H. *Mol. Phys.* **1993**, *80*, 1431.
- $\text{Si}(\text{N}_3)_4$ shows two characteristic IR bands in CH_3CN at 2177 cm^{-1} (vs) and 1333 cm^{-1} (s), which are assigned to the $\nu_{\text{as}}(\text{N}_3)$ and $\nu_{\text{sym}}(\text{N}_3)$ modes, respectively. These bands were not observed in the IR spectra of **1**.
- The ²⁹Si and ¹⁴N NMR chemical shifts are referred to SiMe_4 and CH_3NO_2 .
- Kollwitz, M.; Gauss, J. *Chem. Phys. Lett.* **1996**, *260*, 639.
- Tandura, S. N.; Voronkov, M. G.; Alekseev, N. V. *Top. Curr. Chem.* **1986**, *131*, 99 and references therein.
- The N_{β} signal of **1** ($\delta_{\text{calc}} = -133$ ppm) is hidden under the solvent signal ($\delta = -135.5$ ppm).
- All calculations were carried out with the program system *Turbomole*, V5.3; Ahlrichs, R.; Bär, M.; Häser, M.; Horn, H.; Kölmel, C. *Chem. Phys. Lett.* **1989**, *162*, 165.
- (a) Weigend, F.; Häser, M.; Patzelt, H.; Ahlrichs, R. *Chem. Phys. Lett.* **1998**, *294*, 143. (b) Weigend, F.; Häser, M. *Theor. Chem. Acc.* **1997**, *97*, 331. (c) Schäfer, A.; Huber, C.; Ahlrichs, R. *J. Chem. Phys.* **1994**, *100*, 5829. (d) Eichkorn, K.; Treutler, O.; Ohm, H.; Häser, M.; Ahlrichs, R. *Chem. Phys. Lett.* **1995**, *240*, 283. (e) Eichkorn, K.; Weigend, F.; Treutler, O.; Ahlrichs, R. *Theor. Chem. Acc.* **1997**, *97*, 119.
- Thermal motion in the crystal may produce an apparent shrinkage of the molecular dimensions and is considered by calculating the instantaneous bond lengths, which were estimated with $D_i \approx D_o + (U_B - U_A)/D_o$; *Fundamentals of Crystallography*; Giacovazzo, C., Ed.; IUCr, Oxford University Press: New York, 1992.
- The other bond lengths were less affected (e.g., $D_i(\text{N}_{\alpha}–\text{N}_{\beta})_{\text{av}} = 1.205(2)$ Å) because of the smaller thermal motion of the Si, N_α, and N_β atoms.
- Hirshfeld, F. L. *Acta Crystallogr.* **1976**, *A32*, 239.
- The calculations were carried out with PLATON, v1.04; Spek, A. L. *Acta Crystallogr.* **1990**, *A46*, C34.
- NBO 5.0 Program. Glendening, E. D.; Badenhoop, J. K.; Reed, A. E.; Carpenter, J. E.; Bohmann, J. A.; Morales, C. M.; Weinhold, F., University of Wisconsin, Madison, 2001.
- Heininger, W.; Stucka, R.; Nagorsen, G. Z. *Naturforsch.* **1986**, *B41*, 702.
- Kornath, A. *Angew. Chem., Int. Ed.* **2001**, *40*, 3135.

JA0273187